Dynamic Article Links ▶

View Article Online

PAPER

Synthesis and computational studies of Mg complexes supported by 2,2′:6,2″-terpyridine ligands†

Louise M. Guard,‡ Julio L. Palma,‡ William P. Stratton, Laura J. Allen, Gary W. Brudvig, Robert H. Crabtree, Victor S. Batista* and Nilay Hazari*

The reactions of the substituted 2,2′:6,2″-terpyridine ligands, 4′-mesityl-2,2′:6′,2″-terpyridine (mesitylterpy) (**1a**), 4,4′,4″-tri-*tert*-butyl-2,2′:6′,2″-terpyridine (tri-^{t}Buterpy) (**1b**) and 4′-phenyl-2,2′:6′,2″-terpyridine (phenylterpy) (**1c**) with Grignard reagents were investigated. When half an equivalent of mesitylterpy or tri-^{t}Buterpy were treated with MeMgBr in diethyl ether, the only products were (R-terpy)MgBr$_2$ (R = mesityl (**5a**), or tri-^{t}Bu (**5b**)) and Me$_2$Mg and a similar reaction was observed in THF. Compounds **5a** and **5b** were characterized by X-ray crystallography. Changing the Grignard reagent to PhMgBr also generated **5a** and **5b** along with Ph$_2$Mg, while the reaction between MeMgCl or PhMgCl and **1a** or **1b** generated (R-terpy)MgCl$_2$ (R = mesityl (**6a**), or tri-^{t}Bu (**6b**)) and either Me$_2$Mg or Ph$_2$Mg, respectively. The products from reactions between phenylterpy (**1c**) and Grignard reagents were highly insoluble and could not be fully characterized but appeared to be the same as those from reactions with **1a** and **1b**. In contrast to other studies using tridentate nitrogen ligands, which formed either mixed halide alkyl species or dihalide and bis(alkyl) species depending on whether the Grignard reagent was reacted with the ligand in diethyl ether or THF, the formation of mixed halide, alkyl complexes of the type (R-terpy)MgR′X (R′ = Me or Ph; X = Cl or Br) or dialkyl species such as (R-terpy)MgR′$_2$ (R′ = Me or Ph) was not observed here, regardless of the reaction conditions. DFT studies were performed to complement the experimental studies. The experimental results could not be accurately reproduced unless π-stacking effects associated with free terpyridine were included in the model. When these effects were included, the calculations were consistent with the experimental results which indicated that the formation of the terpy Mg dihalide species and R′$_2$Mg (R′ = Me or Ph) is thermodynamically preferred over the formation of mixed alkyl halide Mg species. This is proposed to be due to the increased steric bulk of the terpy ligand in the coordination plane, compared with other tridentate nitrogen donors.

Introduction

Since the first complexes containing the 2,2′:6,2″-terpyridine (terpy) ligand were prepared in the 1930s,[1–5] this generally κ³-N *meridonal* tridentate ligand has been used extensively to support a range of different coordination compounds.[6,7] In part, this is because terpy is fairly easy to synthesize, inexpensive, oxidation resistant and stable to harsh reaction conditions.[6,7] Electronically, terpy is both a powerful σ-donor, due to its relatively hard nitrogen lone pairs and a reasonable π-acceptor, as a result of the low lying unfilled π*-orbitals of the aromatic rings.[6] Therefore, terpy can support complexes in both low and high oxidation states and terpy containing species have been utilized in a wide variety of applications.[8] These include applications as dye molecules[9] and water oxidation catalysts[10] in solar energy conversion schemes, as metal containing scaffolds for supramolecular[11] and nanoscale[12] chemistry, as reagents for facilitating and studying the kinetics and mechanism of electron transfer in biochemical, inorganic and organic processes[13–15] and as dyes for luminescent sensors[16] and molecular photonic devices.[17,18]

In contrast to the plethora of transition metal complexes containing terpy ligands, examples of s-block metals containing these ligands are very rare.[6] The majority of complexes of this type are either homoleptic species containing two terpy ligands or species containing one terpy ligand and a variable number of water molecules as the remaining ligands.[19–23] Given the importance of organometallic compounds of the s-block (in particular Li and Mg) as reagents in organic synthesis,[24,25] we were interested in preparing organometallic Mg complexes supported by terpy ligands. The synthesis of monomeric derivatives of this

The Department of Chemistry, Yale University, P. O. Box 208107, New Haven, Connecticut 06520, USA. E-mail: victor.batista@yale.edu, nilay.hazari@yale.edu

type could assist in increasing our mechanistic understanding of organic reaction pathways involving Grignard reagents, which are currently difficult to study due to the complex speciation of Grignard reagents in solution.[26] Furthermore, these species could have increased stability compared to other organometallic Mg complexes, which could make them useful as catalysts for lactide polymerization.[27] Here, we show that the reaction of a number of different Grignard reagents (R_2Mg or RMgX) in either diethyl ether or THF with substituted terpy ligands, results in either no reaction or disproportionation to give exclusively non-organometallic products of the form $(terpy)MgX_2$ (X = Cl or Br); these are some of the first Mg complexes supported by terpy ligands. Our results are in direct contrast to reactions between Grignard reagents, such as MeMgBr, and other tridentate nitrogen ligands, which form either mixed halide alkyl complexes, or dihalide and bis(alkyl) complexes depending on whether diethyl ether or THF is used as the solvent.[28,29] Density functional theory is used to understand the binding of the terpy ligand to Mg and explain our experimental observations. Surprisingly, we find that it is crucial to model π-stacking of the terpy ligands in solution to accurately model the energetics of terpy binding to Mg.

Results and discussion

Synthesis and structure of Mg terpyridine complexes

In a series of seminal articles, Parkin and co-workers demonstrated that the treatment of Grignard reagents with protonated tris(pyrazolyl)hydroborates led to a metathesis reaction, in which an alkane was released from the Grignard reagent and a four coordinate Mg species with the tridentate ligand coordinated in a *facial* geometry was formed.[30–34] To the best of our knowledge, the use of Grignard reagents as Mg precursors has only twice been applied to prepare Mg complexes with chelating tridentate neutral ligands.[28,29] Both Steinborn and co-workers and Viebrock and Weiss prepared a mixture of (pmdta)MgBrMe (pmdta = N,N,N',N'',N''-pentamethyldiethylenetriamine), (pmdta)MgMe$_2$ and (pmdta)MgBr$_2$ through the reaction of pmdta with MeMgBr.[28,29] The ratio of the products varied depending on whether the reaction was performed in THF or diethyl ether.[29] We were interested in preparing organometallic Mg complexes supported by terpy ligands. Initially, unsubstituted terpy was treated with MeMgBr in diethyl ether at room temperature and a solid immediately precipitated. Unfortunately, this solid was insoluble in all common solvents and it was not even possible to obtain a ^{1}H NMR spectrum. We postulated that Mg containing

products that were soluble in organic solvents could be generated by adding hydrophobic substituents to the 2,2′:6,2″-terpyridine framework. The coordination chemistry of three different terpy ligands was explored; 4′-mesityl-2,2′:6′,2″-terpyridine (mesitylterpy) (**1a**), commercially available 4,4′,4″-tri-*tert*-butyl-2,2′:6′,2″-terpyridine (tri-^{t}Buterpy) (**1b**) and 4′-phenyl-2,2′:6′,2″-terpyridine (phenylterpy) (**1c**), which was prepared using a literature route.[35]

Initially, the synthesis of mesitylterpy (**1a**) through the reaction of mesityl-chalcone (**2**) with pyridinium iodide (**3**), followed by condensation with ammonium acetate to form mesitylterpy was attempted (eqn (1)). This synthetic protocol has previously been used to construct a variety of different terpyridines[36] but was unsuccessful for mesitylterpy, presumably because steric factors prevented the necessary condensations. The only previously reported synthesis of mesitylterpy (**1a**) by Chen et al.[37] followed the route described by Constable and co-workers for the synthesis of phenylterpy.[35,38] This route involves two steps: (i) the preparation of the diketone (**4**) from 2-acetylpyridine and mesitylaldehyde, which requires a reaction time of four days; and (ii) the formation of the central pyridine ring through condensation of **4** with ammonium acetate. As part of this work, this synthesis was repeated on numerous occasions and no mesitylterpy was formed. However, close inspection of the experimental protocol revealed that Chen and co-workers had utilized 4 equivalents of base in their synthesis of mesitylterpy, whereas Constable *et al.* had only used 1–1.56 equivalents of base in their synthesis of phenylterpy. When the amount of base used in the synthesis of **4** was lowered to 1.56 equivalents, the crude diketone was formed within 12 hours (Scheme 1). Subsequent isolation and purification of **4**, followed by condensation with ammonium acetate allowed us to form mesitylterpy (**1a**) in moderate yield.

As in the analogous reaction with unsubstituted terpy, a solid immediately precipitated out of the reaction mixture when MeMgBr in diethyl ether was treated with mesitylterpy or tri-^{t}-Buterpy. However, after the solid was isolated by filtration, it was soluble in both chlorinated solvents and THF, which allowed for full characterization. Surprisingly, the products of the reaction of one equivalent of our substituted terpy ligands with one equivalent of MeMgBr were half an equivalent of (R-terpy)MgBr$_2$ (R = mesityl (**5a**), or tri-^{t}Bu (**5b**)), which was insoluble in the diethyl ether solution and half an equivalent of Me$_2$Mg, which was soluble in diethyl ether. In addition, an unidentified terpy-containing product was present in low yield (eqn (2)). When half an equivalent of mesitylterpy or tri-^{t}Buterpy was treated with MeMgBr, the only products were **5a** or
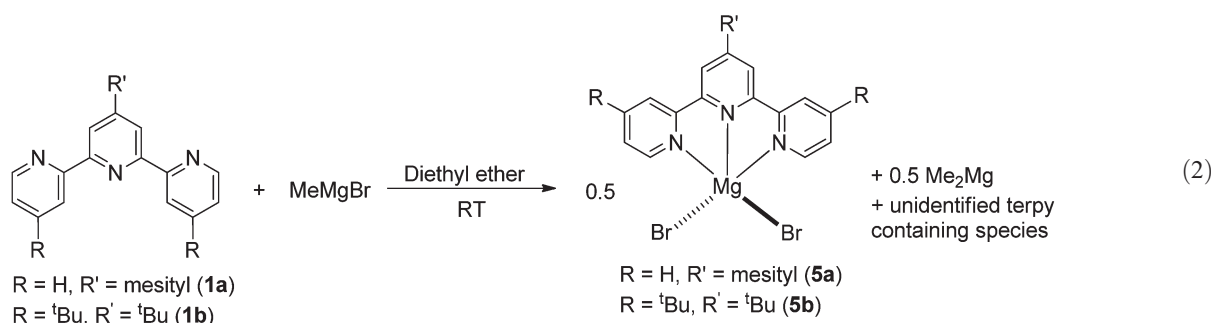
(1)
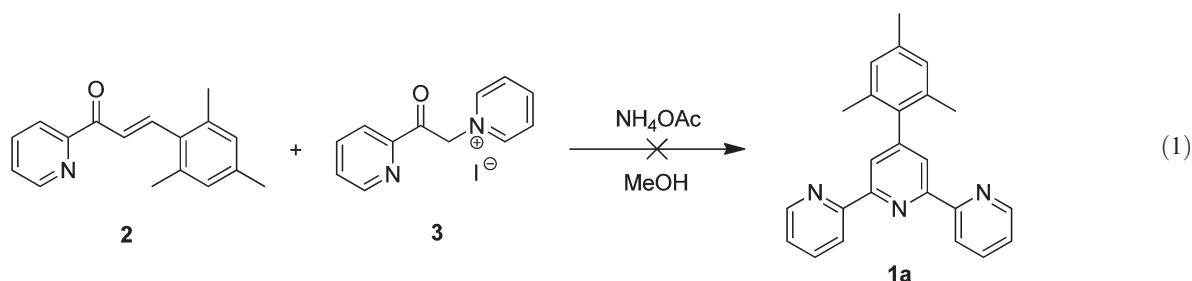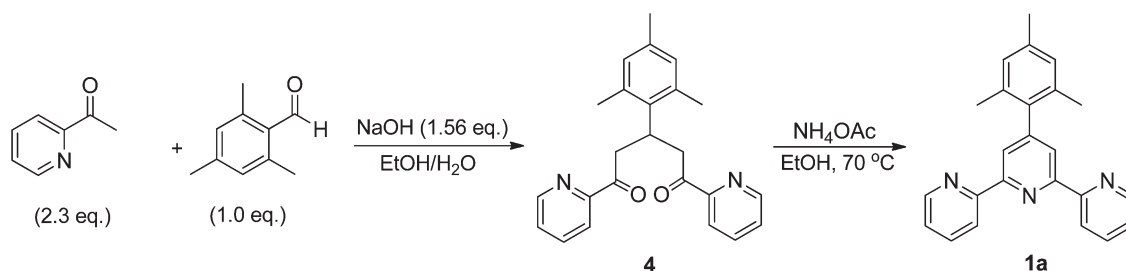
Scheme 1

5b and Me$_2$Mg (eqn (3)). There was no evidence to indicate that mixed halide, alkyl complexes of the type (R-terpy)MgMeBr or dialkyl species such as (R-terpy)MgMe$_2$ were being formed. In fact, when one equivalent of our substituted terpy ligands was added to one equivalent of Me$_2$Mg[39] in diethyl ether or THF, no products containing terpy bound to Mg were isolated and it appeared that if any coordination was occurring, the equilibrium strongly favored free terpy and Me$_2$Mg. Changing the Grignard reagent from MeMgBr to PhMgBr had no effect on reactivity. Again, the only product with terpy coordinated to Mg was (R-terpy)MgBr$_2$, which precipitated from the reaction mixture, and there was no evidence for complexes of the type (R-terpy) MgPhBr or (R-terpy)MgPh$_2$, although free Ph$_2$Mg was observed using ^{1}H NMR spectroscopy. Similarly, when the halide on the Grignard reagent was changed from Br to Cl, the dichloride species **6a** or **6b** was formed (eqn (3)). Complexes **6a** and **6b** were fully characterized. In contrast to reactions with mesityl-terpy and tri-^{t}Buterpy, phenylterpy was too insoluble to give reactions in pure diethyl ether. Adding THF to a diethyl ether solution solubilized the phenylterpy, and it appeared that the phenylterpy coordinated Mg dihalide (**5c**) was formed from the reaction of phenylterpy with MeMgBr. However, compound **5c** was highly insoluble and was only characterized by ^{1}H NMR spectroscopy. The ^{1}H NMR spectrum indicated that a small amount of an unknown impurity was present and **5c** was not isolated in a pure form due to its insolubility.
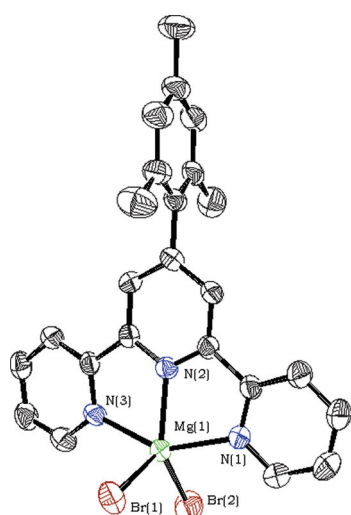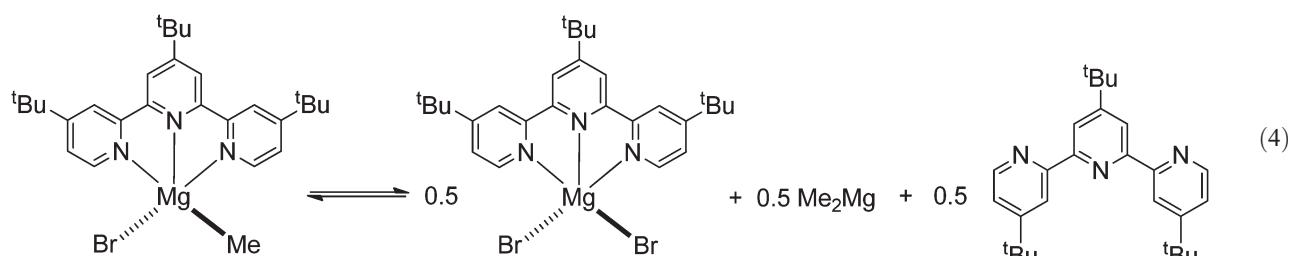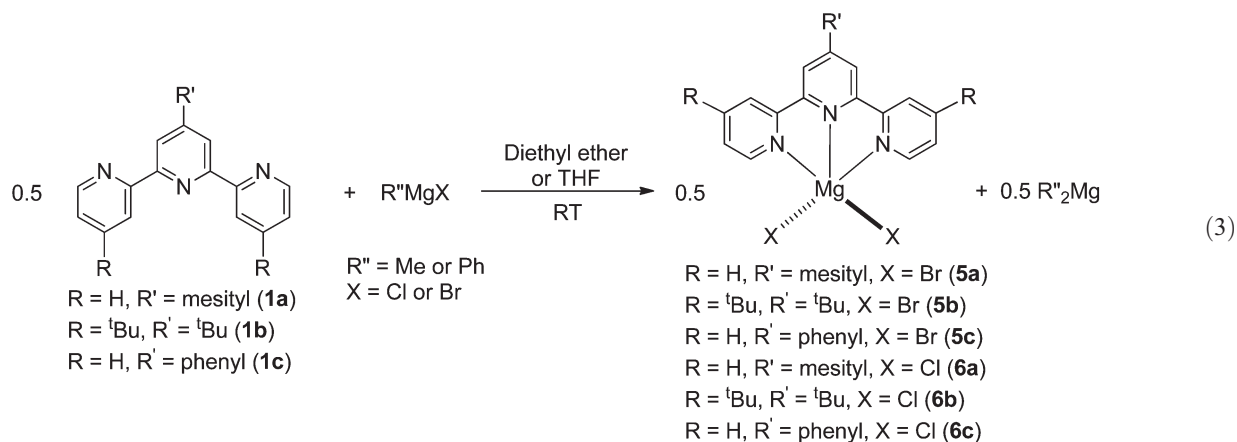
One possible explanation for the selective formation of the dihalide species is that there is an equilibrium between (R-terpy) MgR′X and 0.5 equivalents of (R-terpy)MgX$_2$ and R′$_2$Mg (eqn (4)). If this equilibrium occurs, presumably the insolubility of the dihalide species drives the equilibrium and as a result only the dihalide species is observed (along with the unligated bis(alkyl) species in solution). In order to test this hypothesis, the reaction between half an equivalent of the terpy ligands and

the Grignard reagents was performed in THF, because in this solvent the terpy-coordinated dihalide species, **5a**, **5b**, **6a** and **6b**, are completely soluble. Surprisingly, this reaction also only led to the formation of the ligated dihalide species and the unligated bis(alkyl) species (eqn (3)). In this case, isolation of the terpy Mg dihalide species could be achieved by removing the THF from the reaction mixture and then extracting the bis(alkyl) by-product with diethyl ether. When reactions between Grignard reagents and phenylterpy were performed in THF, ^{1}H NMR spectroscopy indicated that the dihalide species, **5c** and **6c**, were formed. However, the insolubility of **5c** and **6c** precluded full characterization and isolation in a pure form.

The most likely explanation for the selectivity of the reactions between the Grignard reagents and mesitylterpy and tri-^{t}Buterpy is that the terpy Mg dihalide species and the uncoordinated bis (alkyl)Mg species are thermodynamically preferred over the mixed ligand terpy alkylmagnesium halide species. Thus, if any of the terpy alkylmagnesium halide species forms, it rapidly undergoes disproportionation. This is explored further using DFT calculations (*vide infra*). Our results are in direct contrast to Steinborn's finding that, with pmdta as the chelating tridentate nitrogen ligand, the products of the reaction with MeMgBr are influenced by whether the reaction is performed in diethyl ether or THF.[29] In Steinborn's case, the lack of solubility of (pmdta)MgBr$_2$ in diethyl ether drives the reaction to the dihalide and bis(alkyl) products, whereas in THF, where there are no solubility issues, (pmdta)MgMeBr is formed.

The compounds **5a** (Fig. 1) and **5b** (Fig. 2) were characterized by X-ray crystallography. Unsurprisingly, the structures are closely related and in both species the geometry around Mg is distorted trigonal bipyramidal, with the terpy ligand occupying two axial sites and one equatorial site. The bond angle formed by the two nitrogen atoms occupying the axial positions and the Mg center is 146.18(15)° (N(1)–Mg(1)–N(3)) in **5a** and 147.57

$$(2)$$

$$0.5 \quad (1a,\ 1b,\ 1c) \quad + \quad R''MgX \quad \xrightarrow[\text{RT}]{\text{Diethyl ether or THF}} \quad 0.5 \quad (5a\text{–}6c) \quad + \quad 0.5\ R''_2Mg \qquad (3)$$

R" = Me or Ph
X = Cl or Br

R = H, R' = mesityl (**1a**)
R = ^{t}Bu, R' = ^{t}Bu (**1b**)
R = H, R' = phenyl (**1c**)

R = H, R' = mesityl, X = Br (**5a**)
R = ^{t}Bu, R' = ^{t}Bu, X = Br (**5b**)
R = H, R' = phenyl, X = Br (**5c**)
R = H, R' = mesityl, X = Cl (**6a**)
R = ^{t}Bu, R' = ^{t}Bu, X = Cl (**6b**)
R = H, R' = phenyl, X = Cl (**6c**)

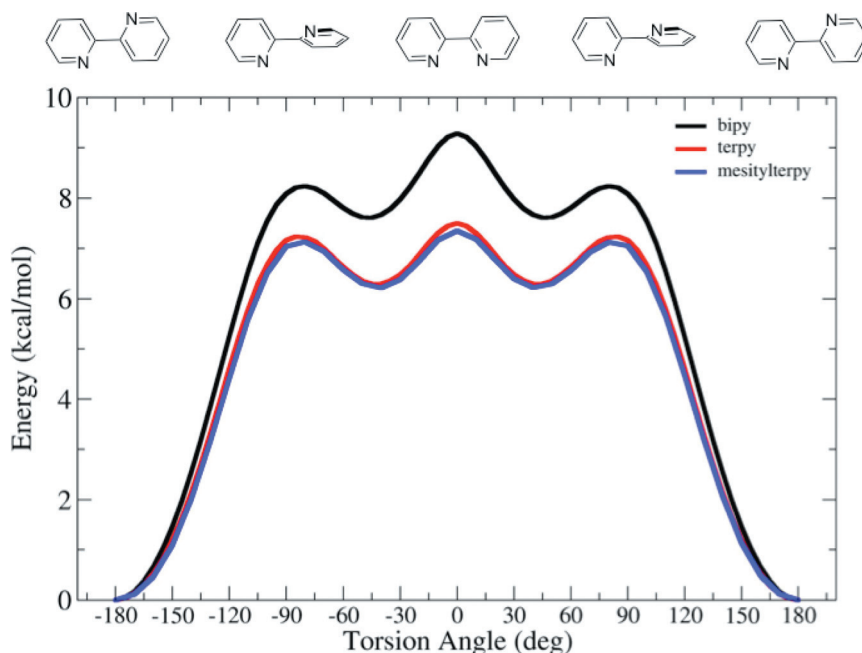$$ \rightleftharpoons \quad 0.5 \quad + \quad 0.5\ Me_2Mg \quad + \quad 0.5 \qquad (4)$$

Fig. 1 X-ray structure of **5a** (hydrogen atoms and solvent in the crystal lattice have been omitted for clarity). Selected bond lengths (Å) and angles (°): Mg(1)–N(1) 2.183(4), Mg(1)–N(2) 2.098(4), Mg(1)–N(3) 2.170(4), Mg(1)–Br(1) 2.4653(18), Mg(1)–Br(2) 2.4435(17), N(1)–Mg(1)–N(2) 73.60(15), N(1)–Mg(1)–N(3) 146.18(15), N(1)–Mg(1)–Br(1) 100.41(13), N(1)–Mg(1)–Br(2) 97.65(12), N(2)–Mg(1)–N(3) 74.06(14), N(2)–Mg(1)–Br(1) 111.22(13), N(2)–Mg(1)–Br(2) 133.96(14), N(3)–Mg(1)–Br(1) 100.23(12), N(3)–Mg(1)–Br(2) 97.62(12), Br(1)–Mg(1)–Br(2) 114.81(6).
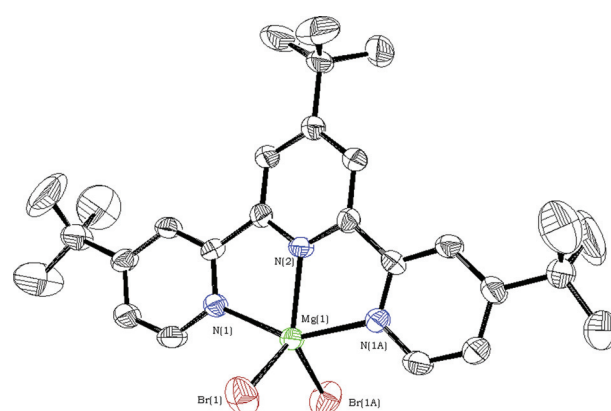
Fig. 2 X-ray structure of **5b** (hydrogen atoms and solvent in the crystal lattice have been omitted for clarity; only one site of disordered *tert*-butyl group shown). Selected bond lengths (Å) and angles (°): Mg(1)–N(1) 2.156(3), Mg(1)–N(2) 2.110(4), Mg(1)–Br(1) 2.4571(14), N(2)–Mg(2)–N(2A) 147.57(11), N(1)–Mg(1)–N(2) 73.78(14), N(1)–Mg(1)–Br(1) 97.97(13), N(1)–Mg(1)–Br(1A) 99.48(9), N(2)–Mg(1)–Br(1) 122.88(4), Br(1)–Mg(1)–Br(2) 114.24(8).

(11)° (N(1)–Mg(1)–N(1A)) in **5b**, indicating a significant distortion from the idealized trigonal bipyramidal geometry. To the best of our knowledge, there are only two other Mg complexes supported by a terpy ligand, Mg(terpy)$_2$$^{2+}$ and Mg(terpy)

Fig. 3 Energy profile for rotation of a single aromatic ring in bipy, terpy and mesitylterpy in the gas phase (lowest energy structure assigned as being at 0 kcal mol^{-1}). Schematic of the torsion angle rotation only depicted for bipy.

Table 1 Torsion energy barriers and local minimum in kcal mol^{-1} for bipy, terpy and mesitylterpy relative to the absolute minimum at 180° for all systems in the gas phase

System	Abs. max. (ϕ)	Loc. max. (ϕ)	Loc. min. (ϕ)
Bipy	9.29(0°)	8.24(80°)	7.60(45°)
Terpy	7.50(0°)	7.23(85°)	6.30(45°)
Mesitylterpy	7.34(0°)	7.12(80°)	6.22(40°)

$(H_2O)_3{}^{2+}$, and these are both six coordinate species with distorted octahedral geometries around Mg.[20,23] Despite the differences in charge and coordination number in **5a** and **5b**, the bond lengths and angles associated with the binding of terpy are comparable with those of the previous two complexes.[20,23] In general, the geometry around the metal center in most five coordinate monomeric Mg complexes is square pyramidal, and examples of trigonal bipyramidal complexes are relatively rare.[40] The structures of **5a** and **5b** are quite different from the structure of (pmdta)MgBr$_2$ which adopts a square pyramidal geometry with one of the Br ligands in the axial position.[29] The difference in geometry may be due to the fact that the pmdta ligand has less in-plane bulk and, thus, allows another ligand to coordinate in the plane.
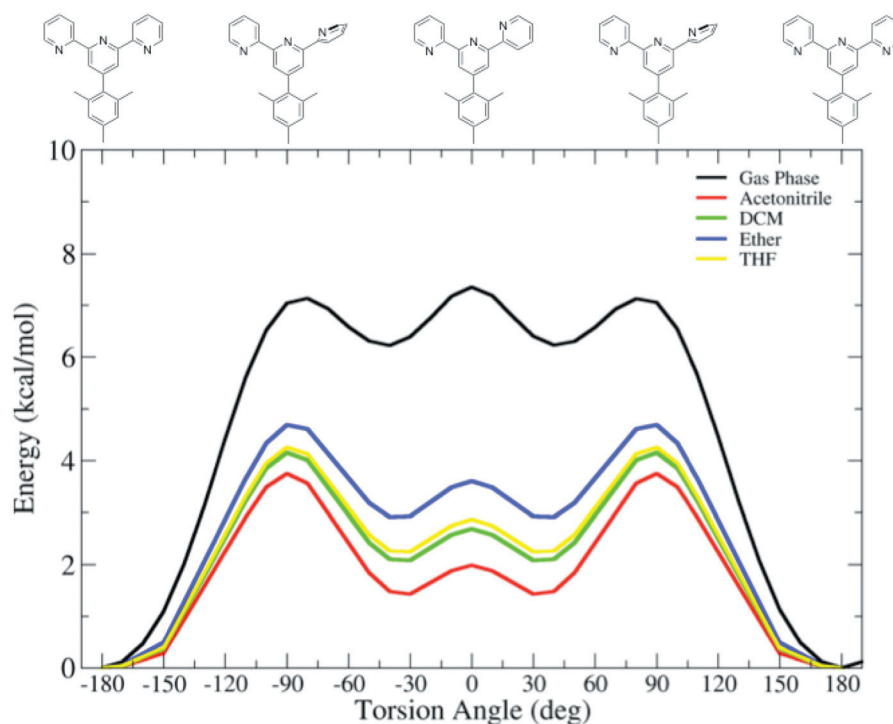
Computational studies on the coordination of terpy to Mg

To gain further insight into the binding of terpy ligands to Grignard reagents, DFT calculations were performed. It has previously been demonstrated that in the most stable conformation of 2,2′-bipyridine (bipy) or terpy, the nitrogen atoms are mutually *anti*.[41,42] In order for coordination to a single metal center to occur, rotation of one ring is required in the case of

bipy, or two rings in the case of terpy. Using DFT (B3LYP/TZV) the energy profiles for rotation of a single ring in bipy, terpy and mesitylterpy were studied. The results are summarized in Fig. 3 and Table 1.

For all three systems, the most stable conformation has a torsion angle (ϕ) between the pyridine rings of 180°. In the case of bipy, there is a local maximum at $\phi = 80°$ (8.24 kcal mol^{-1}), a local minimum at $\phi = 45°$ (7.60 kcal mol^{-1}) and an absolute maximum at $\phi = 0°$ (9.29 kcal mol^{-1}). The torsion angles at which the stationary points are located are similar for terpy and mesitylterpy, although the energy differences between the global minima and the local maxima and minima are smaller. Thus, it only requires approximately 7.5 kcal mol^{-1} to rotate a single ring from the *anti* to *syn* configuration in terpy or mesitylterpy. In both the bipy and terpy cases, the local maximum around 80° $\leq \phi \leq 85°$ is attributed to the break in the conjugation caused by the deviation from planarity, while the absolute maximum at 0° is believed to be caused by both Coulombic repulsion between the lone-pair electrons on the adjacent nitrogen atoms and the creation of an unfavorable net dipole moment in the gas phase of the *syn* conformer. Our results for the bipy system are in agreement with previous calculations performed by Göller and co-workers.[41,42]

We speculated that by changing the polarity of the solvent, the barriers for rotation in the bipy, terpy and mesitylterpy systems could be lowered, along with the absolute difference in energy between the global minima and maxima. A series of calculations were performed in which the energy profiles for rotation were calculated in the presence of solvents with different dielectric constants (the solvent was modelled using the CPCM model). The solvents selected were diethyl ether ($\varepsilon = 4.24$), THF ($\varepsilon = 7.43$), dichloromethane (DCM) ($\varepsilon = 8.93$) and acetonitrile ($\varepsilon = 35.69$). The energy profiles for rotation of a single ring in

Fig. 4 Energy profile for rotation of a single aromatic ring in mesitylterpy in different solvents (lowest energy structure assigned as being at 0 kcal mol^{-1}).
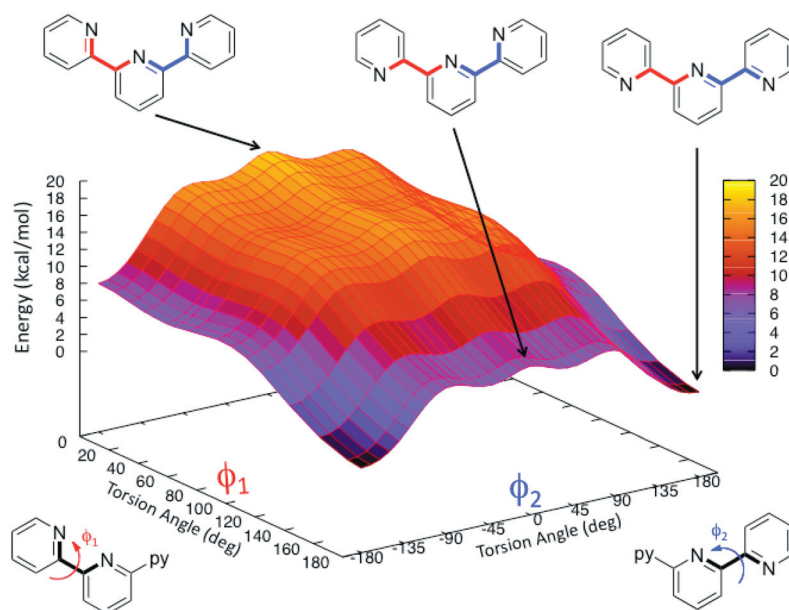
mesitylterpy are shown in Fig. 4, while those for bipy and terpy, which display similar trends are in the ESI.† Our calculations clearly show that the rotational barrier decreases as the polarity of the solvent increases and that the stationary points remain at the same torsion angles. However, the torsion angles at which the global and local maxima are observed have been exchanged. The global maxima is no longer found at $\phi = 0°$ and is instead located between $80° \leq \phi \leq 85°$ depending on the system. This is presumably because the large dipole moment which occurs when $\phi = 0°$ is significantly stabilized in the presence of a solvent (the greater the polarity of the solvent, the greater the stabilization of the dipole), while the smaller dipole which is formed at $\phi \approx 80°$ is stabilized to a lesser extent. Nevertheless, as hypothesized, this partial stabilization leads to a smaller difference between the global minima and maxima in the presence of a solvent. Overall, our results suggest that depending on the strength of the metal precursor solvent interaction, it may be more favorable to coordinate bipy and terpy ligands to a metal in polar solvents.

Surprisingly, rotation of the second terminal ring in terpy is more difficult than rotating the first ring (in this case terpy was used as a model for mesitylterpy due to the computational cost associated with performing these calculations[43]). When a single ring from the ground state *anti, anti* conformation of terpy is rotated to the *anti, syn* conformation, the product is 7.5 kcal mol^{-1} higher in energy than the starting material (Table 1). However, the product with both rings rotated (the *syn, syn* conformation) is 18.5 kcal mol^{-1} higher in energy than the *anti, anti* conformation, indicating that rotation of the second ring is more difficult by approximately 3.5 kcal mol^{-1}. The potential energy surface for rotating both rings in terpy is shown in Fig. 5, where
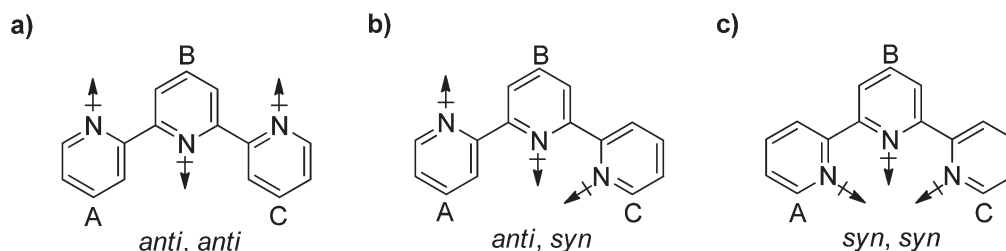
the torsion angle between the central ring and one of the terminal rings, ϕ_1 (red) has been scanned from 0° to 180° and the torsion angle of the second terminal ring, ϕ_2 (blue), has been scanned from −180° to 180°. A torsion angle of 0° corresponds to the *syn* conformation, and 180° and −180° correspond to the *anti* conformation.

We believe that the increased barrier for rotating the second ring in terpy is related to the relative orientation of the dipole moments formed by the three rings (Fig. 6). In the ground state *anti, anti* conformation, the dipole moment of the central ring (B in Fig. 6) is in the opposite direction to the dipole moment of both of the terminal rings (A and C), while the dipole moments of A and C are aligned. When C is rotated from *anti* to *syn* the dipole moment of C becomes partially aligned with the dipole moment of B but is now almost opposite to the dipole moment of A. Thus, the energy lost through the unfavorable alignment of the dipole moment of C and B is partially (but not completely) compensated by the opposite alignment of the dipoles of A and C. Presumably, this also explains why rotation of a single ring in terpy is easier than rotation of a single ring in bipy. When A is rotated, the dipole moment of A is partially aligned with B and fully aligned with the dipole moment of C. Thus two unfavorable alignments of the dipole moments are created, making this process higher in energy than rotation of only one ring, in which only one unfavorable alignment of the dipole moments is created. As for the rotation of a single ring, the barriers for the rotation of the second ring are also lowered depending of the polarity of the solvent, but even in the solvent, rotation of the second ring is more difficult.[43]

The thermodynamic energies for the coordination of mesitylterpy to a variety of different Mg species were calculated based

Fig. 5 Energy surface profile for the rotation of the two aromatic rings in terpy in the gas phase (lowest energy structure assigned as being at 0 kcal mol^{-1}). 0° corresponds to the *syn* conformation while 180° and −180° corresponds to the *anti* conformation. Three representative conformations are shown: *anti*, *anti* being the lowest energy conformation, *anti*, *syn* representing the energy required to rotate a single ring and *syn*, *syn* representing the energy required to rotate both rings. The structures in the bottom of the figure next to the legends represent the initial conformation of each angle and indicate the direction of the rotation.

Fig. 6 Orientation of dipole moments in different isomers of terpy. (a) *anti*, *anti* conformation with dipole moment of rings A and C oriented opposite to B and aligned with each other; (b) *anti*, *syn* conformation with dipole moment of ring A oriented opposite B and partially opposite C and dipole moments of B and C almost aligned; (c) *syn*, *syn* conformation with all dipole moments partially aligned.

Table 2 Thermodynamic energies for the coordination of mesitylterpy to Mg species (eqn (5)). All energies are in kcal mol^{-1} relative to the starting materials

Product	$\Delta H^{\circ}_{(g)}$	$\Delta H^{\circ}_{(ether)}$	$\Delta G^{\circ}_{(g)}$	$\Delta G^{\circ}_{(ether)}$
(mesitylterpy)MgBr$_2$	−1.88	−7.77	−13.24	−19.13
(mesitylterpy)MgBrMe	2.50	−2.58	−8.66	−13.74
(mesitylterpy)MgBrPh	0.04	−4.38	−11.85	−16.28
(mesitylterpy)MgCl$_2$	−0.49	−6.81	−11.11	−17.43
(mesitylterpy)MgClMe	3.39	−1.72	−8.47	−13.57
(mesitylterpy)MgClPh	1.53	−3.18	−9.75	−14.46
(mesitylterpy)MgMe$_2$	6.08	1.12	−6.13	−11.08
(mesitylterpy)MgPh$_2$	2.77	−0.49	−8.25	−11.51

on the assumption that the starting Mg species had two molecules of diethyl ether coordinated to them (eqn (5)). This assumption is consistent with the results of Kato and Mori, who found that the lowest energy structure, for a variety of Grignard reagents in diethyl ether, was a tetrahedral monomer with two

molecules of diethyl ether coordinated.[44] In our case, the two molecules of diethyl ether are released when mesitylterpy coordinates. The energies for the different ligand substitution reactions are summarized in Table 2. In the gas phase, the only reactions which are enthalpically favorable are the coordination of mesitylterpy to (Et$_2$O)$_2$MgBr$_2$ and (Et$_2$O)$_2$MgCl$_2$, while all other reactions are endothermic. However, in the calculated reaction, two molecules in the starting material are being converted into three molecules in the product and, therefore, it is important to include thermal and entropic corrections. The magnitude of the correction is similar in all of the reactions, and the thermodynamic favorability of the reactions is increased by approximately 11 kcal mol^{-1}. Similarly, solvent effects, included using a continuum solvation model,[45,46] also resulted in the reactions becoming more thermodynamically favorable. Unfortunately, once these corrections were applied, our calculated results are no longer consistent with the experimental results. Experimentally, there appears to be no reaction between Me$_2$Mg(OEt$_2$)$_2$ and Ph$_2$Mg(OEt$_2$)$_2$ and mesitylterpy, whereas our calculation with

(5)

R = R' = Cl, Br, Me or Ph
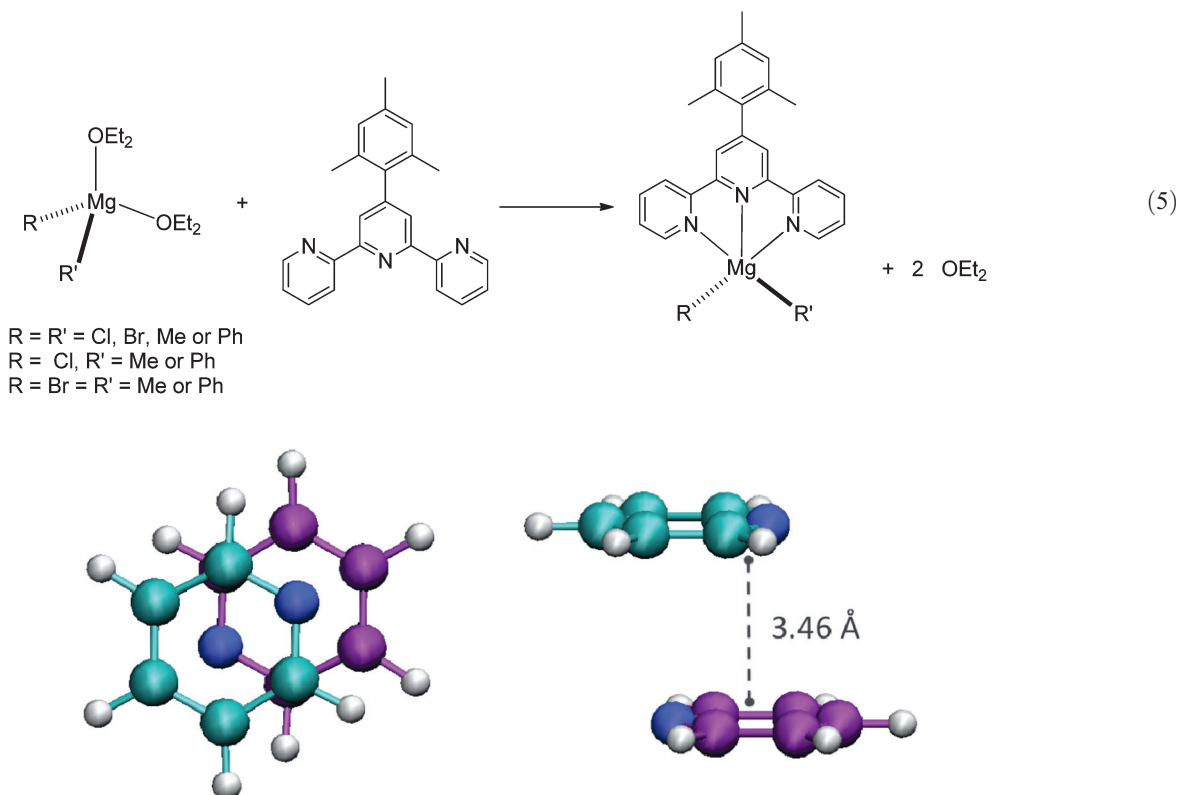R = Cl, R' = Me or Ph
R = Br = R' = Me or Ph

3.46 Å

Fig. 7 Pyridine π-stacking from DFT calculations at the wB97XD level with the 6-31+G(d,p) basis set.

entropic and solvent corrections predicts that this reaction should be favorable by 11 kcal mol^{-1}.
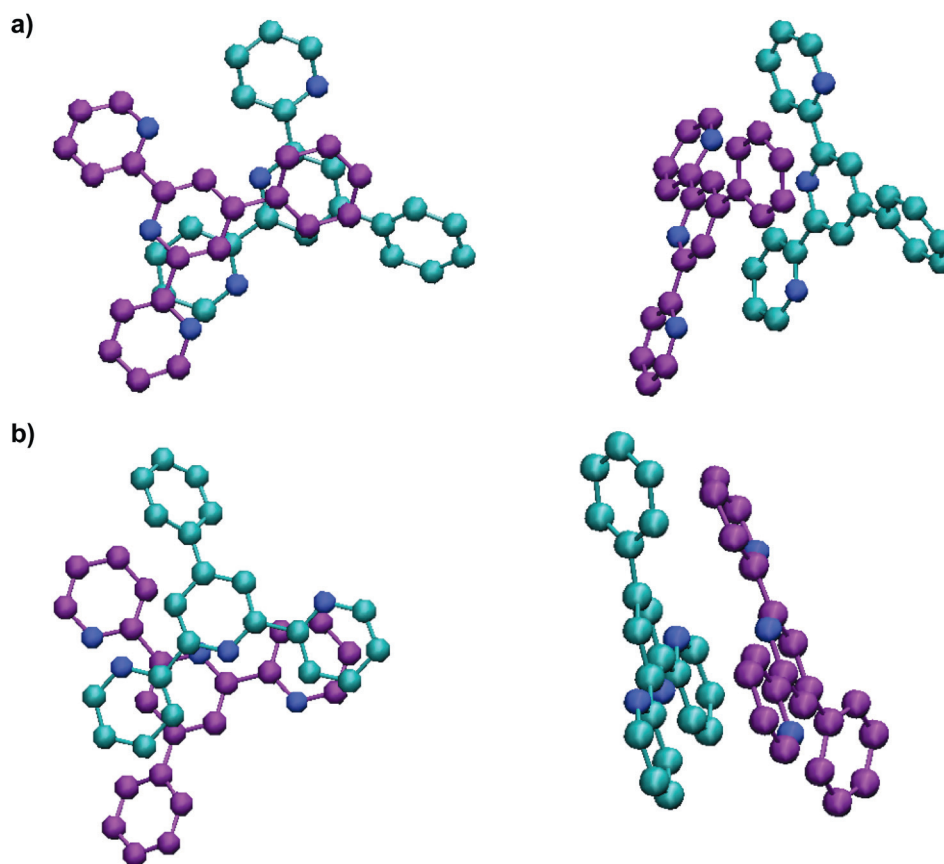
Several possibilities were considered in order to understand the major discrepancy between the computational and experimental results. The assumption that the starting Grignard reagents were monomers was checked and in all cases the monomers were lower in energy than dimeric species with bridging halide or alkyl ligands (see ESI† for more details). Alternatively, it was noted that in the X-ray structure of mesitylterpy, there was a significant π–π interaction[47] between adjacent mesitylterpy units.[48] More specifically the solid state structure showed that the mesityl group forms a strong π–π interaction with one of the nitrogen containing rings of an adjacent mesitylterpy unit.[48] Even though this interaction is presumably weaker in solution, we hypothesized that the presence of such an interaction could be leading to errors in our computational model. Previously, NMR studies have demonstrated that π-stacking is important in solution in phenylacetylene macrocycles[49] and a variety of other aromatic based systems,[50] providing experimental support for our hypothesis.

Traditionally DFT has been poor at modelling weak interactions, such as π-stacking; however, recently developed functionals have been significantly more successful.[51–53] In this study, the functional wB97XD which includes long-range corrections and empirical dispersion was used to model π-stacking.[53] Initially, to assess the accuracy of our method, the interaction between two pyridine dimers was modelled. At the DFT/wB97XD level, with the 6-31+G(d,p) basis set used for all

atoms, the distance between the pyridine rings is 3.46 Å (this is the shortest contact between the ring centroid of one ring and an atom on the other ring) and the stacking energy correction is −3.6 kcal mol^{-1} (where the stacking energy correction is defined as Energy$_{(dimer)}$ − 2Energy$_{(monomer)}$). The optimized structure is shown in Fig. 7 and both the distance between the rings and π-stacking energy are in agreement with those previously reported.[52,54,55] These results suggest that our selected level of theory is appropriate. Using the same method, calculations were performed on phenylterpy and two stable dimeric conformations were found (phenylterpy was used as a model for mesitylterpy because at this higher level of theory it is computationally expensive to calculate two mesitylterpy units). In one conformer, there is π-stacking between the phenyl ring of one monomer and one of the nitrogen rings of the other monomer (Fig. 8). This is the same conformation as observed in the crystal structure of mesitylterpy, and the stacking energy correction was found to be −17.5 kcal mol^{-1}. However, the most stable conformation of two phenylterpy dimers was when both monomers were stacked directly on top of each other so that there was an interaction between two of the three nitrogen containing rings (Fig. 8). In this case, the stacking energy correction was −19.6 kcal mol^{-1}. Presumably, crystal packing effects result in the first conformation being observed in the solid state.

Using our stacking correction energy (assumed to be the same for mesitylterpy as phenylterpy), the thermodynamic data in Table 2 were adjusted, so that we were initially considering a dimeric mesitylterpy starting material (eqn (6)). The crystal

Fig. 8 Phenylterpy π-stacking from DFT calculations at the wB97XD level with the 6-31+G(d,p) basis set. (a) Conformation with interactions between a phenyl group and a nitrogen containing ring with stacking energy correction of −17.5 kcal mol^{-1} and (b) conformation with interactions between two nitrogen containing rings with stacking energy correction of −19.6 kcal mol^{-1}.

Table 3 Thermodynamic energies for the coordination of mesitylterpy to Mg species starting from a dimeric mesitylterpy starting material (eqn (6)). All energies are in kcal mol^{-1} relative to the starting materials

Product	$\Delta G^\circ_{(ether)}$
(mesitylterpy)MgBr$_2$	−9.38
(mesitylterpy)MgBrMe	−3.99
(mesitylterpy)MgBrPh	−6.53
(mesitylterpy)MgCl$_2$	−7.68
(mesitylterpy)MgClMe	−3.82
(mesitylterpy)MgClPh	−4.71
(mesitylterpy)MgMe$_2$	−1.33
(mesitylterpy)MgPh$_2$	−1.76

Table 4 Thermodynamic energies for the equilibrium between mixed alkyl halide Mg mesitylterpy species and dihalide and dialkyl Mg complexes (eqn (7)). All energies are in kcal mol^{-1} relative to the starting materials

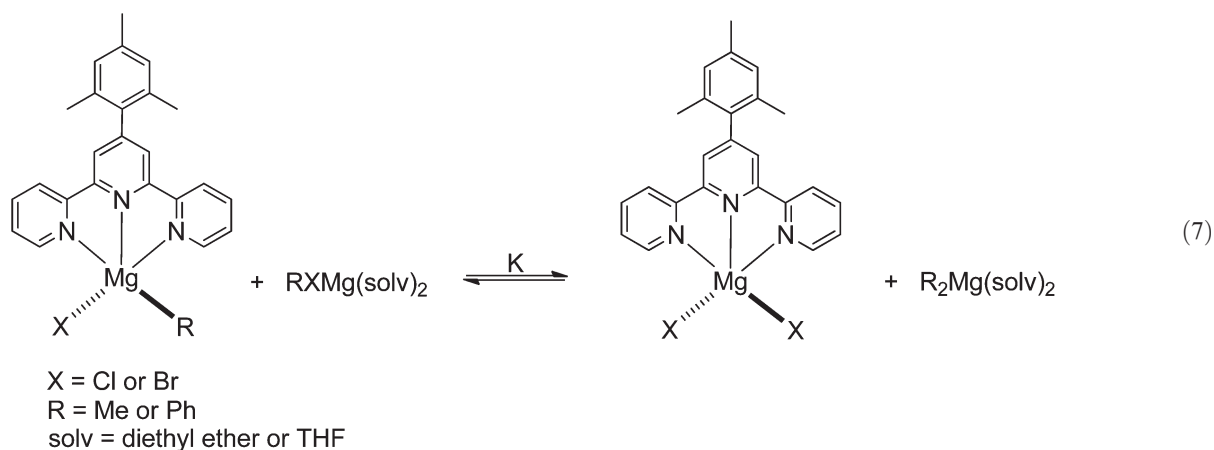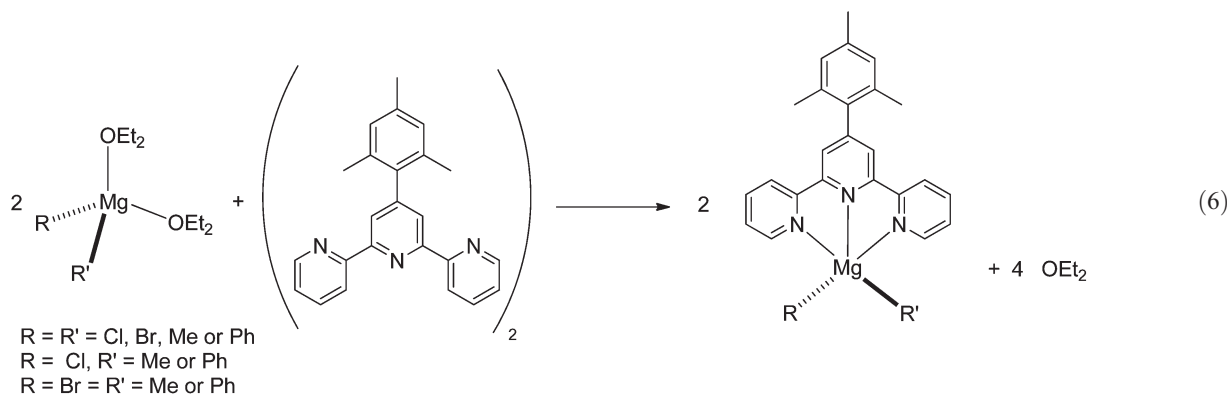| X	R	Solvent	$\Delta G^\circ_{(solv)}$	$K_{(298)}$
Cl	Me	Diethyl ether	0.24	0.66
Cl	Me	THF	1.20	0.13
Cl	Ph	Diethyl ether	0.51	0.42
Cl	Ph	THF	0.41	0.50
Br	Me	Diethyl ether	−0.20	1.4
Br	Me	THF	1.24	0.12
Br	Ph	Diethyl ether	0.57	0.38
Br	Ph	THF	1.81	0.05

structures of the Mg complexes supported by mesitylterpy containing products show no π-stacking (*vide supra*) and, therefore, it was not necessary to make any corrections to the product energies. Our new data are presented in Table 3. It is clear that, by incorporating the effects of π-stacking, the binding of mesitylterpy to Grignard reagents becomes significantly less favorable. Although the Gibbs free energy with solvent corrections is still favorable for the binding of mesitylterpy to Me$_2$Mg(OEt$_2$)$_2$ and Ph$_2$Mg(OEt$_2$)$_2$, these reactions are now favored by only around 1.5 kcal mol^{-1}, and it is probable that our calculated values lie within the DFT error in calculating thermodynamic properties.[56]

Thus, it appears that, in order to obtain consistency between our computational and experimental results, π-stacking effects need to be considered.

One of the most intriguing findings from our experimental results is the selective observation of terpy-coordinated dihalide species and the absence of any mixed alkyl halide complexes when terpy is reacted with Grignard reagents. In order to investigate this selectivity, calculations were performed on the equilibrium shown in eqn (7) in both diethyl ether and THF. The calculated energy differences and equilibrium constants are summarized in Table 4. It can be seen that in almost all cases the

$$2 \; R''' \underset{R'}{\overset{OEt_2}{\underset{|}{Mg}}} OEt_2 \; + \; \left(\text{mesitylterpy} \right)_2 \longrightarrow 2 \; \left(\text{terpy} \right) Mg \; R''' \; R' \; + \; 4 \; OEt_2 \tag{6}$$

R = R' = Cl, Br, Me or Ph
R = Cl, R' = Me or Ph
R = Br = R' = Me or Ph

$$\left(\text{terpy} \right) Mg \underset{R}{\overset{X}{\big|}} + RXMg(solv)_2 \; \underset{}{\overset{K}{\rightleftharpoons}} \; \left(\text{terpy} \right) Mg \underset{X}{\overset{X}{\big|}} + R_2Mg(solv)_2 \tag{7}$$

X = Cl or Br
R = Me or Ph
solv = diethyl ether or THF

mixed alkyl halide species is preferred; however, the energy differences between the two sides are very small. In fact, within the DFT error of calculating thermodynamic properties,[56] it is not possible to say whether the starting material or the product is preferred, and the computational results are not incompatible with the experimental result of only observing the dihalide product (although, in the case of reactions in diethyl ether, the precipitation of the dihalide is presumably an important factor). When the alkyl group on the Grignard is changed from methyl to phenyl, it becomes more favorable to form the mixed alkyl halide species, and this is also true when the solvent is changed from diethyl ether to THF. This suggests that, in order to promote the formation of organometallic Mg complexes supported by terpy ligands, electron deficient alkyl groups may be required. Perhaps the most remarkable aspect of our work is comparing the calculated value of K for the reaction of MeMgBr with mesitylterpy in THF with Steinborn's result for the reaction of MeMgBr with pmdta.[29] Whereas our calculated value is 0.12 (and from experiments it has to be greater than 1), with pmdta Steinborn calculates a value of 1.2×10^{-3}.[29] The difference in equilibrium constant between the two systems is probably related to the change in geometry and indicates that a relatively small change in the nature of the tridentate chelating ligand can cause a large change in the preferred speciation of Mg. Hence, it may be possible to change the nature of the ligand to control the

speciation of the Grignard reagent, in the same way that a solvent is currently used.

Conclusions

Through the reactions of substituted terpy ligands with Grignard reagents, we have prepared rare examples of Mg complexes supported by terpy ligands. Surprisingly, the reactions of the terpy ligands with RMgX (R = Me or Ph; X = Cl or Br) are selective and lead exclusively to products of the type (terpy)MgX$_2$ and R$_2$Mg. The solid state structures of (mesitylterpy)MgBr$_2$ and (tri-^{t}Buterpy)MgBr$_2$ show that the coordination geometry around Mg is distorted trigonal bipyramidal, which is unusual for five coordinate Mg species. A series of DFT calculations, performed to understand the preferential formation of (terpy)MgX$_2$ and R$_2$Mg over (terpy)MgRX, indicated that the reaction could only be modelled accurately if π-stacking effects associated with free terpy were explicitly included. Our combined experimental and theoretical studies suggest that the preference for the formation of (terpy)MgX$_2$ and R$_2$Mg is related to thermodynamic factors. Given that mixed halide alkyl species are the preferred thermodynamic product from the reaction of other tridentate nitrogen containing ligands, such as pmdta with Grignard reagents, this suggests that these types

of ligands can be used to control the speciation of Grignard reagents.

Experimental section

General methods

Experiments were performed under a dinitrogen atmosphere in an M-Braun dry box or using standard Schlenk techniques, unless otherwise noted. (Under standard glovebox conditions, purging was not performed between uses of hexane, diethyl ether, benzene, toluene and THF; thus, when any of these solvents were used, traces of all these solvents were in the atmosphere and could be found intermixed in the solvent bottles.) Moisture- and air-sensitive liquids were transferred by stainless steel cannula on a Schlenk line or in a dry box. Solvents were dried by passage through a column of activated alumina followed by storage under dinitrogen. All commercial chemicals were used as received, except where noted. PhMgCl in THF, 2,2′:6′,2″-terpyridine and 4,4′,4″-tri-*tert*-butyl-2,2′:6′,2″-terpyridine (**1b**) were purchased from Aldrich, MeMgBr in THF and PhMgBr in both Et$_2$O and THF were purchased from Acros Organics and MeMgCl in THF from Alfa Aesar. Deuterated solvents were obtained from Cambridge Isotope Laboratories. CD$_2$Cl$_2$ was dried using CaH$_2$ and C$_6$D$_6$ using sodium metal. Both were vacuum-transferred prior to use. NMR spectra were recorded on Bruker AMX-400 and -500 spectrometers at ambient probe temperatures. Chemical shifts are reported in ppm with respect to residual internal protio solvent for ^{1}H and ^{13}C {^{1}H} NMR spectra; *J* values are given in Hz. Robertson Microlit Laboratories, Inc., performed the elemental analyses. Literature procedures were utilized to synthesize pyridinium iodide (**3**)[57] and phenylterpy[35,38] (**1c**) and a modified literature procedure was used to synthesize mesityl-chalcone (**2**) (mesitylaldehyde was used instead of *para*-nitrobenzaldehyde).[58]

X-ray crystallography

The diffraction experiments were carried out on a Rigaku Mercury275R CCD (SCX mini) diffractometer with a sealed tube at 223 K using graphite-monochromated Mo Kα radiation (λ = 0.710 73 Å). The software used was SMART for collecting frames of data, indexing reflections, and determination of lattice parameters, SAINT for integration of intensity of reflections and scaling, SADABS for empirical absorption correction, and SHELXTL for space group determination, structure solution, and least-squares refinements on |*F*|. The crystals were mounted at the end of glass fibers and used for the diffraction experiments. Anisotropic thermal parameters were refined for the rest of the non-hydrogen atoms. Hydrogen atoms were placed in their ideal positions. Details of the crystal and refinement data for **5a** and **5b** are given in the ESI.†

Synthesis and characterization of compounds

Mesitylterpy (1)

Preparation of intermediate of 3-mesityl-1,5-di(pyridin-2-yl) pentane-1,5-dione (4). 2-acetylpyridine (0.89 ml, 7.79 mmol),

mesityl aldehyde (0.50 ml, 3.37 mmol) and sodium hydroxide (210 mg, 5.25 mmol) were combined in a 25 ml round-bottom flask containing a stir bar and ethanol–water (3.5 ml/2.5 ml). The reaction was stirred at 35–40 °C for 12 hours, during which time the color changed to purple. After 12 hours, water (100 ml) and dichloromethane (100 ml) were added and the solution was transferred to a separatory funnel. The organic layer was washed with water (3 × 100 ml) and brine (1 × 100 ml), and dried over sodium sulfate before being evaporated *in vacuo*. The crude mixture was purified using silica gel by flash column chromatograph (0–30% EtOAc in hexanes as eluent) to give **4** as an oil (605 mg, 49% yield).

^{1}H NMR (CD$_2$Cl$_2$, 400.0 MHz): δ 8.62 (2H, ddd, Ar*H*, *J* = 4.76, 1.67, 0.93 Hz), 7.93 (2H, dt, Ar*H*, *J* = 7.85, 0.87 Hz), 7.77 (2H, td, Ar*H*, *J* = 7.60, 1.74 Hz), 7.41 (2H, ddd, Ar*H*, *J* = 7.52, 4.76, 1.22), 6.79 (1H, s, Ar*H*), 6.74 (1H, s, Ar*H*), 4.68 (1H, m, MesC*H*R$_2$), 3.77 (4H, m, COC*H*$_2$), 2.55 (3H, s, ArC*H*$_3$), 2.45 (3H, s, ArC*H*$_3$), 2.19 (3H, s, ArC*H*$_3$).

Synthesis of mesitylterpy (1) from 4. Mesityl-dione (**4**) (605 mg, 1.62 mol) and ammonium acetate (663 mg, 8.61 mmol) were refluxed in ethanol (5 ml) in a 10 ml round-bottom flask for 12 hours. The solution changed color from yellow to green during this time. The reaction was cooled to RT and a cream colored solid crashed out when the solvent was concentrated under reduced pressure. The resulting solid was isolated by filtration to give crude mesitylterpy. Further purification using basic alumina column chromatography (2.5% EtOAc in hexanes as eluent) gave **1** as a white powder (272 mg, 45% yield). The overall yield for the two steps is 22%.

^{1}H NMR data were analogous to those previously reported.[37]

(mesitylterpy)MgBr$_2$ (5a). Mesitylterpy (0.10 g, 0.29 mmol) was added to a Schlenk flask, dissolved in diethyl ether (25 ml) and a solution of PhMgBr in diethyl ether (2.8 M, 0.21 ml, 0.57 mmol) added. The immediate precipitation of a pale green solid was observed and the mixture stirred for one hour at RT. The reaction mixture was filtered and the solid dried under reduced pressure to yield **5a** as an off white solid. Yield: 0.125 g (82%). Diffraction-quality crystals were grown by diffusion of diethyl ether into a concentrated dichloromethane solution. This reaction could also be performed using MeMgBr as the Grignard reagent or using THF as the solvent.

^{1}H NMR (CD$_2$Cl$_2$, 400.0 MHz): δ 9.13 (2H, d, Ar*H*, *J* = 4.81 Hz), 8.14 (4H, m, Ar*H*), 8.09 (2H, s, Ar*H*), 7.73 (2H, m, Ar*H*), 7.06 (2H, s, Ar*H*), 2.38 (3H, s, ArC*H*$_3$), 2.10 (6H, s, ArC*H*$_3$). ^{13}C-{^{1}H} NMR (CD$_2$Cl$_2$, 125.8 MHz): δ 158.1 (s), 152.3 (s), 151.4 (s), 150.1 (s), 140.9 (s), 139.6 (s), 135.4 (s), 135.1 (s), 129.3 (s), 127.6 (s), 123.5 (s), 122.0 (s), 21.39 (s), 21.0 (s). Anal. found (calcd for C$_{24}$H$_{21}$Br$_2$MgN$_3$·CH$_2$Cl$_2$): C 48.4 (48.4), H 4.2 (3.8), N 6.3 (6.7) %. Note one molecule of CH$_2$Cl$_2$ was found in the crystal structure and in the ^{1}H NMR spectrum (see ESI† for spectrum).

(tri-^{t}Buterpy)MgBr$_2$ (5b). A PhMgBr solution in diethyl ether (2.8 M, 0.18 ml, 0.50 mmol) was added to a Schlenk flask containing a solution of tri-^{t}Buterpy (0.10 g, 0.25 mmol) in diethyl ether (25 ml), causing instantaneous precipitation of a blue solid. The suspension was then stirred for 1 hour at RT. After filtering, the solid was dried under vacuum to afford **5b** as a pale blue

powder. Yield: 0.136 g (93%). Diffraction-quality crystals were grown by diffusion of pentane into a dichloromethane solution. This reaction could also be performed using MeMgBr as the Grignard reagent or using THF as the solvent.

^{1}H NMR (CD$_2$Cl$_2$, 500.0 MHz): δ 8.98 (2H, dd, Ar*H*, *J* = 5.52, 0.62 Hz), 8.20 (2H, s, Ar*H*), 8.16 (2H, dd, Ar*H*, *J* = 1.68, 0.57 Hz), 7.69 (2H, dd, Ar*H*, *J* = 5.54, 1.77 Hz), 1.55 (9H, s, ArC(C*H*$_3$), 1.46 (18H, s, ArC(C*H*$_3$). ^{13}C-\{^{1}H\} NMR (CD$_2$Cl$_2$, 125.8 MHz): δ 168.5 (s), 165.6 (s), 152.1 (s), 150.9 (s), 150.31 (s), 124.6 (s), 118.9 (s), 118.6 (s), 36.7 (s), 36.1 (s), 30.8 (s), 30.7 (s). Anal. found (calcd for C$_{27}$H$_{35}$Br$_2$MgN$_3$): C 55.1 (55.4), H 5.9 (6.0), N 7.0 (7.2) %.

(phenylterpy)MgBr$_2$ (5c). Phenylterpy (0.10 g, 0.32 mmol) was dissolved in THF (25 ml) and a solution of PhMgBr in THF (1 M, 0.65 ml, 0.65 mmol) added. The solution was initially yellow and turned green after 3 minutes of stirring, followed by precipitation of a light green solid. The mixture was stirred for 2 hours at RT and filtered. The solid residue was washed with 2 × 25 ml diethyl ether, though an impurity remained and the product was not cleanly isolated due to its insolubility. This reaction could also be performed using MeMgBr as the Grignard reagent or using a mixture of diethyl ether and THF as the solvent.

^{1}H NMR (CD$_2$Cl$_2$, 400.0 MHz): δ 9.14 (2H, d, Ar*H*, *J* = 4.51 Hz), 8.41 (2H, s, Ar*H*), 8.32 (2H, d, Ar*H*, *J* = 8.02 Hz), 8.16 (2H, td, Ar*H*, *J* = 7.73, 1.62), 7.85 (2H, m, Ar*H*), 7.74 (2H, ddd, Ar*H*, *J* = 7.44, 4.94, 0.59), 7.63 (3H, m, Ar*H*).

(mesitylterpy)MgCl$_2$ (6a). A solution of PhMgCl in THF (2.0 M, 0.14 ml, 0.29 mmol) was added to a solution of mesitylterpy (0.05 g, 0.14 mmol) in THF (20 ml). The yellow solution turned green within minutes. After 1 hour of stirring at RT, the solvent was removed *in vacuo* to give a green oil. The oil was washed with 2 × 15 ml diethyl ether, to give **6a** as a light yellow solid. Yield: 0.049 g (78%). This reaction could also be performed using MeMgCl as the Grignard reagent.

^{1}H NMR (CD$_2$Cl$_2$, 400.0 MHz): δ 9.08 (2H, d, Ar*H*, *J* = 5.08 Hz), 8.14 (4H, m, Ar*H*), 8.07 (2H, s, Ar*H*), 7.72 (2H, m, Ar*H*), 7.06 (2H, s, Ar*H*), 2.37 (3H, s, ArC*H*$_3$), 2.09 (6H, s, ArC*H*$_3$).^{13}C-\{^{1}H\} NMR (CD$_2$Cl$_2$, 125.8 MHz): δ 157.9 (s), 152.5 (s), 151.2 (s), 150.4 (s), 140.8 (s), 139.5 (s), 135.4 (s), 135.2 (s), 129.3 (s), 127.5 (s), 123.4 (s), 121.8 (s), 21.39 (s), 21.0 (s). Anal. found (calcd for C$_{24}$H$_{21}$Cl$_2$MgN$_3$): C 61.2 (64.5), H 3.8 (4.7), N 8.6 (9.4) %. Note despite repeated attempts a satisfactory elemental analysis could not be obtained for this compound. The ^{1}H NMR spectrum is included in the ESI† to demonstrate that this species was synthesized in high purity.

(tri-^{t}Buterpy)MgCl$_2$ (6b). Tri-^{t}Buterpy (0.10 g, 0.25 mmol) was dissolved in THF (25 ml) and a solution of PhMgCl in THF (2.0 M, 0.25 ml, 0.50 mmol) added *via* syringe. After one hour stirring at RT, the solvent was removed to give a blue oil which was washed with 1 × 15 ml diethyl ether. The resulting solid was dried *in vacuo* to give **6b** as a light blue powder. Yield: 0.124 g (90%). This reaction could also be performed using MeMgCl as the Grignard reagent.

^{1}H NMR (CD$_2$Cl$_2$, 500.0 MHz): δ 8.92 (2H, dd, Ar*H*, *J* = 5.42, 0.32 Hz), 8.19 (2H, s, Ar*H*), 8.16 (2H, dd, Ar*H*, *J* = 1.75, 0.32 Hz), 7.68 (2H, dd, Ar*H*, *J* = 5.48, 1.75 Hz), 1.55 (9H, s,

ArC(C*H*$_3$), 1.46 (18H, s, ArC(C*H*$_3$). ^{13}C-\{^{1}H\} NMR (CD$_2$Cl$_2$, 125.8 MHz): δ 168.3 (s), 165.4 (s), 152.3 (s), 150.8 (s), 150.6 (s), 124.5 (s), 118.9 (s), 118.5 (s), 36.6 (s), 36.1 (s), 30.8 (s), 30.7 (s). Anal. found (calcd for C$_{27}$H$_{35}$Cl$_2$MgN$_3$·0.5CH$_2$Cl$_2$): C 60.8 (61.3), H 6.4 (6.7), N 7.5 (7.8) %. Note half a molecule of CH$_2$Cl$_2$ was observed in the ^{1}H NMR spectrum after recrystallization from a diethyl ether–dichloromethane solution (see ESI† for spectrum).

(phenylterpy)MgCl$_2$ (6c). A solution of PhMgCl in THF (2.0 M, 0.32 ml, 0.65 mmol) was added to a solution of phenylterpy (0.10 g, 0.32 mmol) in THF (25 ml). The initially yellow solution turned green within minutes, followed by precipitation of a green solid. After filtration, the solid was washed with 2 × 25 ml THF though an unknown impurity remained and the product was not cleanly isolated due to its insolubility. This reaction could also be performed using MeMgCl as the Grignard reagent.

^{1}H NMR (CD$_2$Cl$_2$, 500.0 MHz): δ 9.08 (2H, d, Ar*H*, *J* = 4.63 Hz), 8.39 (2H, s, Ar*H*), 8.30 (2H, d, Ar*H*, *J* = 7.99 Hz), 8.14 (2H, td, Ar*H*, *J* = 7.43, 1.65), 7.85 (2H, m, Ar*H*), 7.72 (2H, m, Ar*H*), 7.63 (3H, m, Ar*H*).

Computational procedures

All calculations were performed using the Gaussian 09 Revision A.02 package.[59] Electronic structure calculations were performed with density functional theory (DFT) using the Becke3–Lee–Yang–Parr (B3LYP) functional.[60,61] The TZV basis set was used for Mg, C, O, and H atoms while the 6-311++g(d,p) was used for the halogen atoms, Cl and Br. This level of theory and the basis sets were selected after comparing bond lengths and angles in the crystal structure of (mesitylterpy)MgBr$_2$ with the optimized structures from calculations using a number of different functionals and basis sets. Electronic structure calculations consisted of geometry optimizations, frequency calculations and solvent effect calculations to obtain enthalpies and free energies of reactions in gas phase and in solution. Free energies of reactions were obtained using the Born–Haber thermodynamic cycle where the optimized structures in gas phase were used to calculate the zero-point correction energy and entropic contribution *via* a vibrational frequency calculation. Solvation free energies were obtained with the self-consistent reaction field (SCRF) for the standard continuum solvation model (CPCM) using the optimized structures and the thermodynamic correction from the gas phase calculations.[45,46] Stacking energies of the phenylterpy were performed with the wB97XD level of DFT[53] and 6-31+G (d,p) basis set. Benchmark calculations were performed on pyridine where π-stacking interactions have been widely studied and reported.

Acknowledgements

References

1 G. T. Morgan and F. H. Burstall, *J. Chem. Soc.*, 1932, 20.
2 G. T. Morgan and F. H. Burstall, *J. Chem. Soc.*, 1934, 1498.
3 G. T. Morgan and F. H. Burstall, *J. Chem. Soc.*, 1937, 1649.
4 G. T. Morgan and F. H. Burstall, *J. Chem. Soc.*, 1938, 1675.
5 G. T. Morgan and G. R. Davies, *J. Chem. Soc.*, 1938, 1858.
6 E. C. Constable, *Adv. Inorg. Chem.*, 1986, **30**, 69.
7 R. P. Thummel, Terpyridine, oligopyridine, and polypyridine ligands, in *Comprehensive Coordination Chemistry II*, ed. J. A. McCleverty and T. J. Meyer, Elsevier, New York, 2004, vol.1, pp. 41–53.
8 S. D. Cummings, *Coord. Chem. Rev.*, 2009, **253**, 449.
9 M. K. Nazeeruddin, P. Péchy, T. Renouard, S. M. Zakeeruddin, R. Humphry-Baker, P. Comte, P. Liska, L. Cevey, E. Costa, V. Shklover, L. Spiccia, G. B. Deacon, C. A. Bignozzi and M. Grätzel, *J. Am. Chem. Soc.*, 2001, **123**, 1613.
10 J. Limburg, J. S. Vrettos, L. M. Liable-Sands, A. L. Rheingold, R. H. Crabtree and G. W. Brudvig, *Science (Washington, D. C.)*, 1999, **283**, 1524.
11 E. C. Constable, *Prog. Inorg. Chem.*, 1994, **42**, 67.
12 A. Winter, S. Hoeppener, G. R. Newkome and U. S. Schubert, *Adv. Mater.*, 2011, **23**, 3484.
13 A. Juris, V. Balzani, F. Barigelletti, S. Campagna, P. Belser and A. von Zelewsky, *Coord. Chem. Rev.*, 1988, **84**, 85.
14 R. Langen, I. J. Chang, J. P. Germanas, J. H. Richards, J. R. Winkler and H. B. Gray, *Science (Washington, D. C.)*, 1995, **268**, 1733.
15 E. Baranoff, J.-P. Collin, L. Flamigni and J.-P. Sauvage, *Chem. Soc. Rev.*, 2004, **33**, 147.
16 K. M.-C. Wong and V. W.-W. Yam, *Acc. Chem. Res.*, 2011, **44**, 424.
17 A. Harriman and R. Ziessel, *Chem. Commun.*, 1996, 1707.
18 S. Flores-Torres, G. R. Hutchison, L. J. Soltzberg and H. D. Abruña, *J. Am. Chem. Soc.*, 2006, **128**, 1513.
19 E. C. Constable, M. J. Doyle, J. Healy and P. R. Raithby, *J. Chem. Soc., Chem. Commun.*, 1988, 1262.
20 E. C. Constable, J. Healy and M. G. B. Drew, *Polyhedron*, 1991, **10**, 1883.
21 T. W. Bell, P. J. Cragg, M. G. B. Drew, A. Firestone and D.-I. A. Kwok, *Angew. Chem., Int. Ed.*, 1992, **31**, 345.
22 B. W. Skelton, A. F. Waters and A. H. White, *Aust. J. Chem.*, 1996, **49**, 137.
23 A. F. Waters and A. H. White, *Aust. J. Chem.*, 1996, **49**, 147.
24 *Grignard Reagents: New Developments*, ed. H. G. Richey Jr., Wiley, Chichester, 2000.
25 B. J. Wakefield, *Organomagnesium Methods in Organic Synthesis*, Academic Press, London, 1995.
26 K. C. Cannon and G. R. Krow, The composition of grignard reagents in solution: the schlenk equilibrium and its effect on reactivity. in *Handbook of Grignard Reagents*, ed. G. S. Silverman and P. E. Rakita, Marcel Decker, New York, 1996, pp. 271–289.
27 C. A. Wheaton, P. G. Hayes and B. J. Ireland, *Dalton Trans.*, 2009, 4832.
28 H. Viebrock and E. Weiss, *J. Organomet. Chem.*, 1994, **464**, 121.
29 R. I. Yousef, B. Walfort, T. Rüffer, C. Wagner, H. Schmidt, R. Herzog and D. Steinborn, *J. Organomet. Chem.*, 2005, **690**, 1178.
30 R. Han, A. Looney and G. Parkin, *J. Am. Chem. Soc.*, 1989, **111**, 7276.
31 R. Han, M. Bachrach and G. Parkin, *Polyhedron*, 1990, **9**, 1775.
32 R. Han and G. Parkin, *J. Am. Chem. Soc.*, 1990, **112**, 3662.
33 R. Han and G. Parkin, *Organometallics*, 1991, **10**, 1010.
34 R. Han and G. Parkin, *J. Am. Chem. Soc.*, 1992, **114**, 748.
35 E. C. Constable, J. Lewis, M. C. Liptrot and P. R. Raithby, *Inorg. Chim. Acta*, 1990, **178**, 47.
36 G. A. Koohmareh and M. Sharifi, *J. Appl. Polym. Sci.*, 2010, **116**, 179.
37 H. Chen, R. Tagore, S. Das, C. D. Incarvito, J. W. Faller, R. H. Crabtree and G. W. Brudvig, *Inorg. Chem.*, 2005, **44**, 7661.
38 S. A. Moya, R. Pastene, H. L. Bozec, P. J. Baricelli, A. J. Pardey and J. Gimeno, *J. Inorg. Chim. Acta*, 2001, **312**, 7.
39 C. R. Noller and W. R. White, *J. Am. Chem. Soc.*, 1937, **59**, 1354.
40 D. A. Fletcher, R. F. McMeeking and D. Parkin, *J. Chem. Inf. Comput. Sci.*, 1996, **36**, 746.
41 A. H. Göller and U.-W. Grummt, *Chem. Phys. Lett.*, 2000, **321**, 399.
42 A. H. Göller and U.-W. Grummt, *Chem. Phys. Lett.*, 2002, **354**, 233.
43 See ESI† for more details.
44 T. Mori and S. Kato, *J. Phys. Chem. A*, 2009, **113**, 6158.
45 V. Barone and M. Cossi, *J. Phys. Chem. A*, 1998, **102**, 1995.
46 M. Cossi, N. Rega, G. Scalmani and V. Barone, *J. Comput. Chem.*, 2003, **24**, 669.
47 C. Janiak, *J. Chem. Soc., Dalton Trans.*, 2000, 3885.
48 W. Leslie, A. S. Batsanov, J. A. K. Howard and J. A. G. Williams, *Dalton Trans.*, 2004, 623.
49 A. S. Shetty, J. Zhang and J. S. Moore, *J. Am. Chem. Soc.*, 1996, **118**, 1019.
50 C. A. Hunter, K. R. Lawson, J. Perkins and C. J. Urch, *J. Chem. Soc., Perkin Trans. 2*, 2001, 651.
51 Y. Zhao and D. G. Truhlar, *Phys. Chem. Chem. Phys.*, 2005, **7**, 2701.
52 M. Piacenza and S. Grimme, *ChemPhysChem*, 2005, **6**, 1554.
53 J.-D. Chai and M. Head-Gordon, *Phys. Chem. Chem. Phys.*, 2008, **10**, 6615.
54 P. Mignon, S. Loverix, F. D. Proft and P. Geerlings, *J. Phys. Chem. A*, 2004, **108**, 6038.
55 B. Bezbaruah, P. Hazarika, A. Gogoi, O. Medhi and C. Medhi, *J. Biophys. Chem.*, 2011, **2**, 32.
56 S. E. Wheeler, A. Moran, S. N. Pieniazek and K. Houk, *J. Phys. Chem. A*, 2009, **113**, 10376.
57 S. H. Wadman, J. M. Kroon, K. Bakker, R. W. A. Havenith, G. P. M. van Klink and G. van Koten, *Organometallics*, 2010, **29**, 1569.
58 G. A. Koohmareh and M. Sharifi, *J. Appl. Polym. Sci.*, 2010, **116**, 179.
59 M. J. Frisch, G. W. Trucks, H. B. Schlegel, G. E. Scuseria, M. A. Robb, J. R. Cheeseman, G. Scalmani, V. Barone, B. Mennucci, G. A. Petersson, H. Nakatsuji, M. Caricato, X. Li, H. P. Hratchian, A. F. Izmaylov, J. Bloino, G. Zheng, J. L. Sonnenberg, M. Hada, M. Ehara, K. Toyota, R. Fukuda, J. Hasegawa, M. Ishida, T. Nakajima, Y. Honda, O. Kitao, H. Nakai, T. Vreven, J. A. Montgomery, Jr., J. E. Peralta, F. Ogliaro, M. Bearpark, J. J. Heyd, E. Brothers, K. N. Kudin, V. N. Staroverov, R. Kobayashi, J. Normand, K. Raghavachari, A. Rendell, J. C. Burant, S. S. Iyengar, J. Tomasi, M. Cossi, N. Rega, J. M. Millam, M. Klene, J. E. Knox, J. B. Cross, V. Bakken, C. Adamo, J. Jaramillo, R. Gomperts, R. E. Stratmann, O. Yazyev, A. J. Austin, R. Cammi, C. Pomelli, J. Ochterski, R. L. Martin, K. Morokuma, V. G. Zakrzewski, G. A. Voth, P. Salvador, J. J. Dannenberg, S. Dapprich, A. D. Daniels, O. Farkas, J. B. Foresman, J. V. Ortiz, J. Cioslowski and D. J. Fox, *GAUSSIAN 09 (Revision A.2)*, Gaussian, Inc., Wallingford, CT, 2009.
60 A. D. Becke, *J. Chem. Phys.*, 1993, **98**, 5648.
61 A. D. Becke, *J. Chem. Phys.*, 1993, **98**, 1372.